

NANO EXPRESS

Open Access

Vanadia supported on nickel manganese oxide nanocatalysts for the catalytic oxidation of aromatic alcohols

Syed F Adil¹, Saad Alabbad¹, Mufsir Kuniyil¹, Mujeeb Khan¹, Abdulrahman Alwarthan¹, Nils Mohri², Wolfgang Tremel², Muhammad Nawaz Tahir^{2*} and Mohammed Rafiq Hussain Siddiqui^{1*}

Abstract

Vanadia nanoparticles supported on nickel manganese mixed oxides were synthesized by co-precipitation method. The catalytic properties of these materials were investigated for the oxidation of benzyl alcohol using molecular oxygen as oxidant. It was observed that the calcination temperature and the size of particles play an important role in the catalytic process. The catalyst was evaluated for its oxidation property against aliphatic and aromatic alcohols, which was found to display selectivity towards aromatic alcohols. The samples were characterized by employing scanning electron microscopy, transmission electron microscopy, X-ray diffraction, Brunauer-Emmett-Teller analysis, thermogravimetric analysis, and X-ray photoelectron spectroscopy.

Keywords: Catalysis; Vanadia nanoparticles; Mixed metal oxide

Background

Catalysis, which is largely a surface phenomenon, is an area of research that has been a widely studied subject by scientists and technologists [1-4]. However, the zeal for finding a better performing catalyst for various processes including CO oxidation [5], Fischer-Tropsch synthesis [6], MOFs for biomimetic catalysis [7], fuel cell reactions [8], and selective hydrogenolysis of aryl ethers [9] still is an ongoing process. Among several elements that are being tested and tried for catalysis, vanadium oxide and other compounds containing vanadium have attracted significant attention as catalyst for many oxidation reactions [10-14]. Apart from this, vanadium oxide has also been explored for various other applications including pseudocapacitors [15] and cathode material [16] in various conversion reactions of alkanes to alkenes, organic acids, and the synthesis of light olefins by means of oxidative dehydrogenation (ODH) [17-22]. Furthermore, the catalytic oxidation properties of vanadium-based catalysts have also been extensively exploited for several other

reactions such as conversion of propane to CO_x/H₂ [23], propane partial oxidation [24], oxidation of SO₂ [25], formaldehyde to formic acid [26], oxidation of α -hydroxy ketones, α -hydroxy esters [27], aerobic oxidative cleavage of secondary-tertiary glycols [28], and oxidative dehydrogenation of ethane [29]. In some cases, it has also been used as support material for other catalysts, e.g., Pt nanoparticles, supported by vanadia-decorated carbon nanotubes for methanol electro-oxidation reaction [30]. Notably, vanadium has displayed excellent catalytic activities in all forms, whether it has been employed as a supported active phase or in the form of mixed oxides prepared in combination with other ions; it displayed efficient catalytic properties as an oxidation catalyst.

Recently, mixed metal oxides (MMO) have attracted significant attention as solid catalysts, due to their low cost, easy regeneration, selective action, and excellent acid-base redox properties [31]. Among various MMO, manganese-based MMO have attracted much attention due to their higher catalytic performances [32]. Several catalytic reactions using manganese-oxide-based MMO have been reported. Examples include the catalytic reaction of hydrogen production via autothermal reforming of ethanol [33], steam reforming of tar from biomass pyrolysis [34], methane combustion at low temperature

* Correspondence: tahir@uni-mainz.de; rafiqs@ksu.edu.sa

²Institute for Inorganic and Analytical Chemistry, University of Mainz, Duesbergweg 10-14, 55128 Mainz, Germany

¹Department of Chemistry, College of Science, King Saud University, P.O. 2455, Riyadh 11451, Kingdom of Saudi Arabia

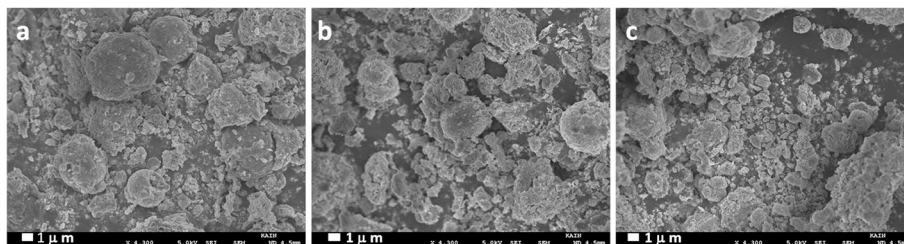


Figure 1 SEM of the catalyst (a) V_2O_5 (1%)-NiMnO, (b) V_2O_5 (3%)-NiMnO, and (c) V_2O_5 (5%)-NiMnO at 300°C.

[35], and enhanced glucose electrooxidation [36] carried out using nickel manganese MMO. Our group has been involved in the synthesis of various MMOs [37] and evaluated their catalytic performance for several organic transformations [38]. In this study, to exploit the excellent catalytic activity of vanadium oxide, we report the synthesis of heterogeneous catalysts based on vanadium oxide nanoparticles supported on nickel manganese oxide MMO. The as-prepared catalysts were characterized using various spectroscopic and microscopic techniques including transmission electron microscopy (TEM), scanning electron microscopy (SEM), X-ray diffraction (XRD), X-ray photoemission spectroscopy (XPS), and thermogravimetric analysis (TGA), and their catalytic activities were evaluated for the oxidation of various aromatic alcohols.

Methods

Preparation of vanadium oxide supported on nickel manganese oxide by deposition method

Ninety-five milliliters of 0.2 M solutions of nickel nitrate and manganese nitrate were mixed in a round-bottomed flask, followed by addition of 10 mL of 0.2 M solution of vanadium chloride. The resulting solution was heated to 80°C under stirring using a mechanical stirrer. A 1 M solution of $NaHCO_3$ was added dropwise until the solution attained a pH 9. The solution was continuously stirred at the same temperature for about 3 h and left on stirring over night at room temperature. The solution was filtered using a Buchner funnel under vacuum and then dried at 70°C overnight. The product obtained was characterized using SEM, TEM, EDAX, XRD, XPS,

Brunauer-Emmett-Teller (BET), and TGA. The resulting powder was then calcined at different temperatures and evaluated for its oxidation activity for the oxidation of benzyl alcohol as a model precursor.

Catalyst testing

In a typical reaction, 300 mg of catalyst was loaded in a glass flask pre-charged with 0.2 mL (2 mmol) benzyl alcohol mixed with 10 mL toluene as a solvent; the mixture was then refluxed at 100°C, and oxygen was bubbled at a flow rate of 20 mL min^{-1} into the mixture under vigorous stirring. After reaction, the solid catalyst was separated by centrifugation, and the liquid samples were analyzed by gas chromatography to evaluate the conversion of the desired product using an Agilent 7890A GC (Agilent Technologies, Inc., Santa Clara, CA, USA), equipped with a flame ionization detector (FID) and a 19019S-001 HP-PONA column.

Catalyst characterization

SEM and elemental analysis (energy-dispersive X-ray analysis (EDX)) were carried out using a Jeol SEM model JSM 6360A (JEOL Ltd., Akishima-shi, Japan). This was used to determine the morphology of nanoparticles and its elemental composition. TEM was carried out using a Jeol TEM model JEM-1101 (JEOL Ltd., Akishima-shi, Japan), which was used to determine the shape and size of nanoparticles. Powder X-ray diffraction studies were carried out using an Altima IV (Make: Rigaku, Shibuya-ku, Japan) X-ray diffractometer. Fourier transform infrared spectroscopy (FT-IR) spectra were recorded as KBr pellets using a PerkinElmer 1000 FT-IR spectrophotometer

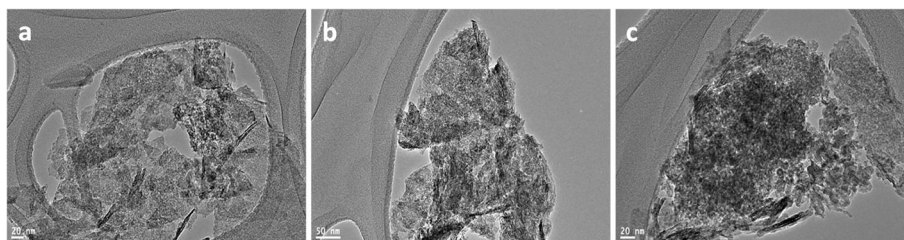


Figure 2 TEM of the catalyst (a) V_2O_5 (1%)-NiMnO, (b) V_2O_5 (3%)-NiMnO, and (c) V_2O_5 (5%)-NiMnO at 300°C.

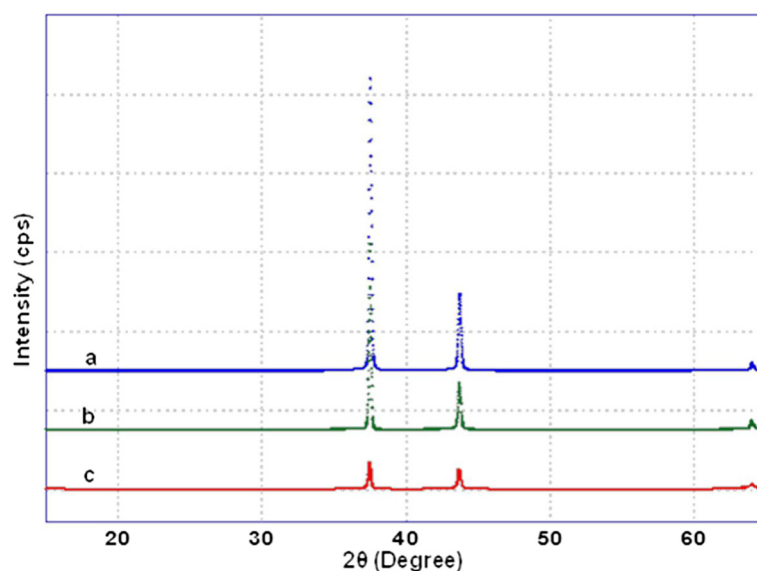


Figure 3 XRD pattern of catalyst (a) V_2O_5 (1%)-NiMnO, (b) V_2O_5 (3%)-NiMnO, and (c) V_2O_5 (5%)-NiMnO calcined 300°C .

(PerkinElmer, Waltham, MA, USA). BET surface area was measured on a NOVA 4200e surface area and pore size analyzer (Quantachrome Instruments, FL, USA). Thermogravimetric analysis was carried out using PerkinElmer Thermogravimetric Analyzer 7 (PerkinElmer, Waltham, MA, USA). XPS was measured on a PHI 5600 Multi-Technique XPS (Physical Electronics, Lake Drive East, Chanhassen, MN, USA) using monochromatized Al $K\alpha$ at 1486.6 eV. Peak fitting was performed with CASA XPS Version 2.3.14 software.

Results and discussion

Catalyst characterization

The morphology and the particle size of the synthesized catalyst were characterized using SEM and TEM. The SEM micrographs of the pre-calcined (300°C) catalyst V_2O_5 ($X\%$)-NiMnO, where $X = (1, 3, \text{ and } 5)$, are shown in Figure 1. It was observed that the morphology of the synthesized catalysts is not well defined, and the surface appears to be rugged without any obvious phase separation. The stoichiometric amount of elements was confirmed from the EDX analysis and found to be approximately in agreement with the calculated value.

The TEM image of the catalyst V_2O_5 ($X\%$)-NiMnO ($X = 1, 3, 5$) was carried out to investigate the shape and size of the particles more closely (Figure 2). The average particle size was calculated using image-processing program Image J software of the image adjacent to it. It was found that the synthesized catalyst 1% and 3% V_2O_5 -NiMnO possessed particle sizes of 2.8 and 2.7 nm, respectively, whereas V_2O_5 (5%)-NiMnO was found to contain particles of size 2.2 nm. The TEM image analysis

of the other synthesized catalysts gave information of the particles to be around 3 to 4 nm in size.

XRD spectrum

Figure 3 shows X-ray diffraction patterns of mixed oxides of nickel manganese with different % of vanadium oxide nanoparticles pre-calcined at 300°C . The structural results are listed in Table 1. The analysis of the XRD spectrum of $X\%$ V_2O_5 -NiMnO (Figure 3), where $X = (1, 3, \text{ and } 5)$ of pre-calcined at 300°C showed that the V_2O_5 (1%)-NiMnO, V_2O_5 (3%)-NiMnO, and V_2O_5 (5%)-NiMnO contain reflections corresponding to cubic hexanickel manganese (IV) oxide (ICSD # 40584). No reflection corresponding to vanadium oxide was observed which could be due to the low percentage present in the catalyst.

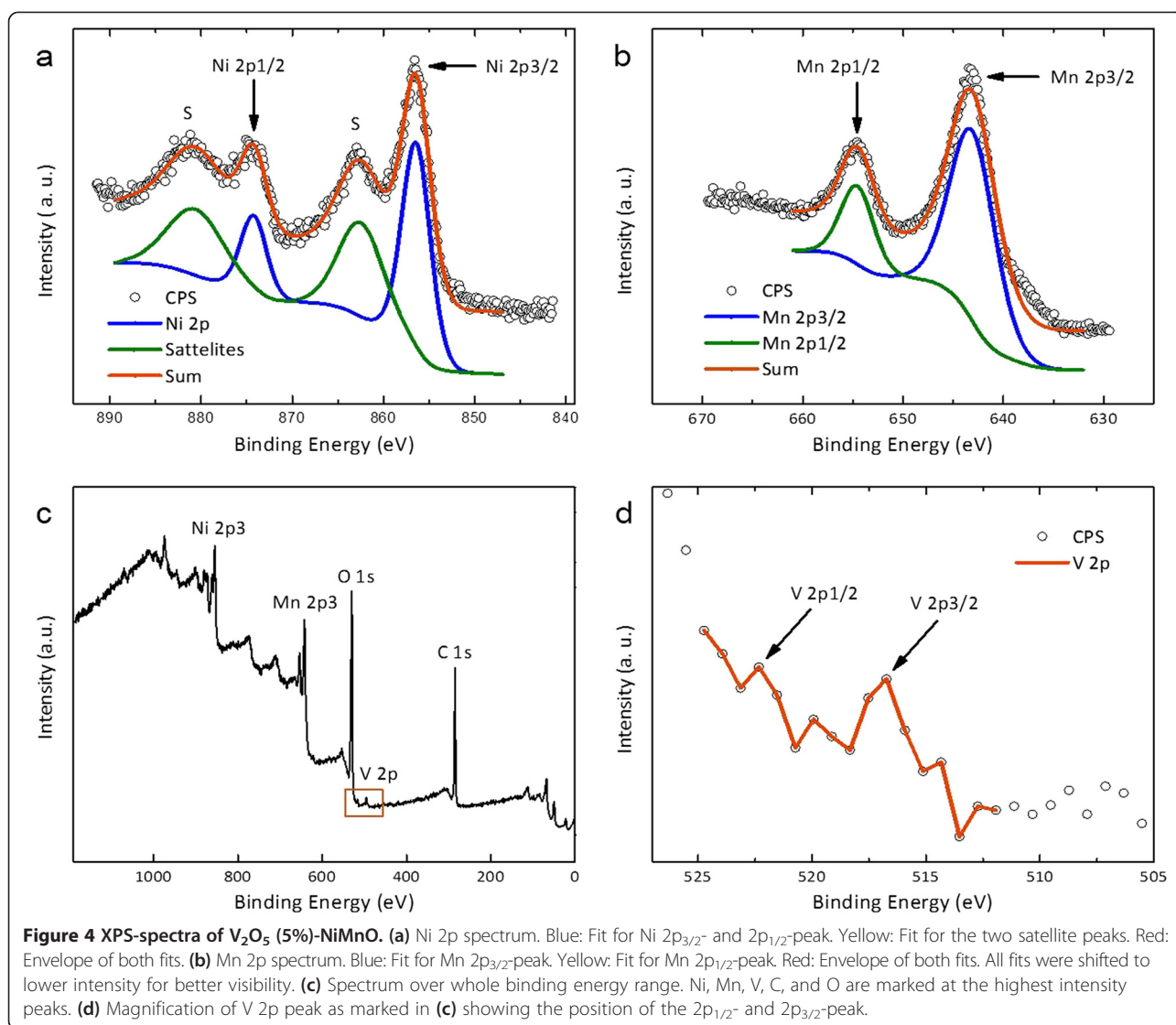
XPS analysis

The distinct amount of vanadium oxide supported on the surface region and the oxidation state of the vanadium were confirmed using XPS studies. The spectrum

Table 1 Textural and structural properties of vanadium-oxide-doped nickel manganese oxide

Sample	Loading [wt%]	Calcination temperature ($^\circ\text{C}$)	S_{BET}	D [nm]	Phase
$1V_2O_5$	1	300	68.28	14.477	Ni_3MnO_4
$3V_2O_5$	3	300	62.81	12.269	Ni_3MnO_4
$5V_2O_5$	5	300	98.54	20.804	Ni_3MnO_4
$5V_2O_5$	5	400	57.00	16.908	Ni_3MnO_4
$5V_2O_5$	5	500	20.97	12.326	Ni_3MnO_4

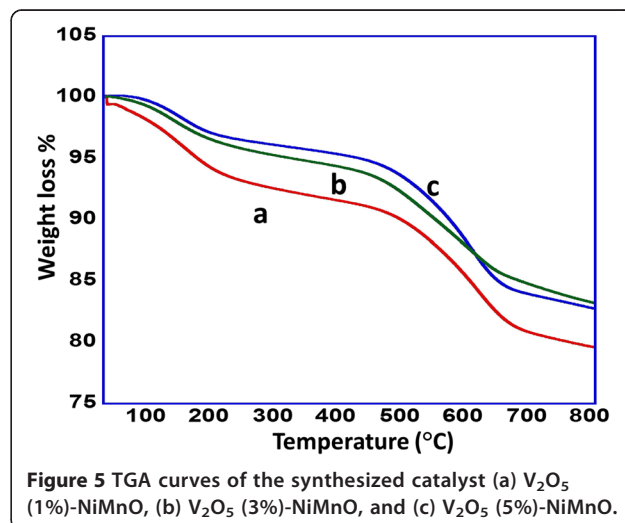
S_{BET} is the specific surface area. D is the crystal domain size calculated by using Scherrer Equation. Phase detected by XRD.

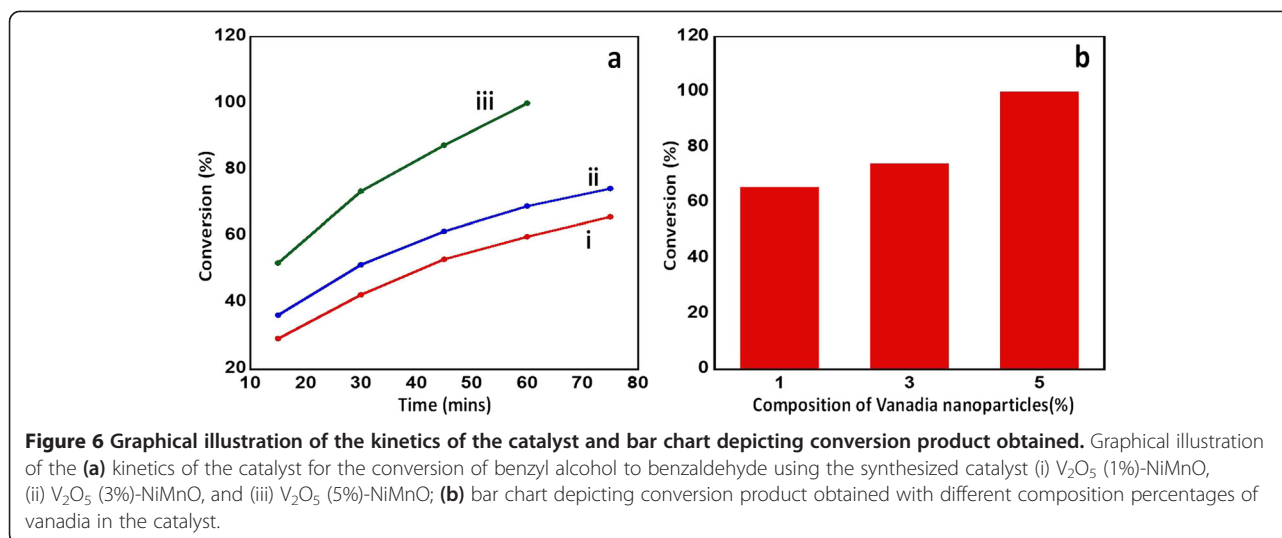


is given in Figure 4. It was also intended to establish the phase changes if any on the surface of the catalytic system before and after catalyzing the oxidation reaction. It was observed that there is no significant change in the spectrum obtained for the catalysts before and after reaction. Two weak signals observed at a binding energy (BE) of 517.0 and 522.4 eV indicate that the oxidation state of +5 for vanadium is present in the catalyst, which agree well with the results published by Silversmit et al. [39]. The very low percentage amount of vanadium

Table 2 Binding energies of transition metal compounds calculated from the maxima in the XPS spectra

Compound	$BE_1(2p_{1/2})$ (eV)	$BE_2(2p_{3/2})$ (eV)	$\Delta E (BE_1 - BE_2)$ (eV)
Vanadium	522.25	516.95	5.20
Manganese	654.77	643.46	11.31
Nickel	874.47	856.63	17.84





could be responsible for the weak signal. The binding energies obtained for manganese and nickel (see Table 2) suggest that the oxidation states are +4 and +2, respectively [40,41], which corroborates the results obtained from the XRD. There was no change observed in the binding energies corresponding to the manganese and nickel after the reaction indicating that there is no change in oxidation state of the metals.

From the above results, it can be concluded the oxidation property of the mixed metal oxides used is not related to the redox properties of the transition metals used but could be a surface phenomenon.

Thermogravimetric studies

The thermal stability of the as synthesized catalyst with different % loading of vanadium oxide nanoparticles were studied using TGA analysis. Temperature was programmed from 25°C to 800°C at a heating rate of 10°C min⁻¹. It was observed that almost all the synthesized catalysts are thermally stable, yielding a maximum loss of weight of 20.23% at 800°C found in the case of 1% V_2O_5 -nanoparticle-loaded catalyst making it to be the least thermally stable among the synthesized catalysts, while the catalysts with 3% V_2O_5 and 5% V_2O_5 can be assumed to be the most thermally

Table 3 Effect of calcination temperature on the catalytic properties

Entry	Catalyst	Temperature (°C)	Conversion (%)	Selectivity (%)
1	NiMnO	400	52.56	<99
2	V_2O_5 (5%)-NiMnO	300	100	<99
3	V_2O_5 (5%)-NiMnO	400	30	<99
4	V_2O_5 (5%)-NiMnO	500	8	<99

Reaction conditions: amount of catalyst 300 mg; reaction temperature 100°C; oxygen flow rate 20 mL min⁻¹; benzyl alcohol 2 mmol; toluene 10 mL; reaction time 3 h.

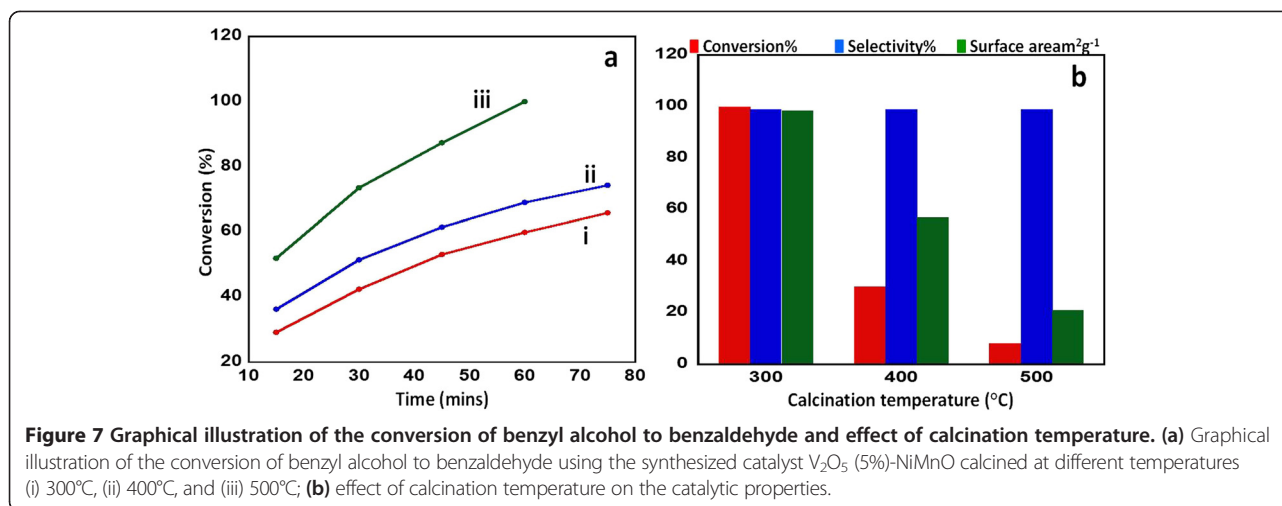
stable catalysts with a least weight loss % of just 16.5% and 17.2%, respectively, at 800°C. A graphical illustration is given in Figure 5.

Evaluation of catalytic properties

Optimization of percentage of Vanadium oxide nanoparticles and calcination temperature

In order to ascertain the percentage composition of vanadium oxide nanoparticles to be supported on the nickel-manganese-mixed oxide for the best catalytic performance as an oxidation catalyst, a series of catalysts with varying percentages of vanadium oxide nanoparticles were synthesized and evaluated for their catalytic property, monitoring the oxidation of benzyl alcohol to benzaldehyde as a model reaction. The reaction was carried out at 100°C, while passing molecular O_2 gas as a source of oxygen. During the study, a trend of steady increase in performance of the synthesized catalyst was observed with the increase in the composition percentage of vanadium oxide, which explains the influence of vanadium oxide nanoparticles on the catalytic performance. The catalyst with 1% and 3% vanadium oxide yielded 65.77% and 74.27% conversion product, respectively, within 75 min, while the catalyst with 5% vanadium oxide nanoparticles yielded 100% conversion product within the same time. In order to understand the effect of presence of vanadium oxide nanoparticles, a similar reaction was carried out in the presence of the catalyst without the vanadium oxide nanoparticles (i.e., NiMnO) which yielded a 52.56% conversion product. This indicated that vanadium oxide acts as a promoter for the selective catalytic oxidation.

The kinetics of the reaction were studied by collecting the sample in regular intervals of 15 min and subjected to gas chromatography from which the percentage conversion was calculated. It was observed that the catalyst with 1% and 3% V_2O_5 start of by giving 30% and 37%



conversion product, respectively, in the first 15 min of the reaction time. However, as the reaction proceeds, the rate slows down, and after 75 min, there was very slight change in the conversion product obtained; hence, the reaction was not carried further. But the catalyst with 5% V_2O_5 yields about 52% conversion product in the first 15 min and gradually proceeds to the 100% conversion in 60 min. From this, it can be clearly stated that there is a promoter effect on the catalytic performance of the catalyst by incorporating vanadium oxide nanoparticles. The selectivity in all the above reactions was found to be >99%. A graphical illustration is given in Figure 6.

Calcination temperature has an effect on the surface area and porosity, which in turn affects the catalytic performance as reported by Al-Fatesh and coworker [42]. In order to establish the above mentioned effect of

calcination temperature on the synthesized catalyst, V_2O_5 (5%)-NiMnO catalyst, which yielded 100% conversion product in the earlier study, was taken and was calcined at different temperatures, i.e., 300°C, 400°C, and 500°C. Under similar reaction conditions, the conversion of benzyl alcohol to benzaldehyde was carried out. It was observed that with the catalyst V_2O_5 (5%)-NiMnO calcined at 300°C the reaction starts off by yielding a 51% conversion product in the first 15 min of the reaction time and yields a 100% conversion product within 60 min, while the catalyst calcined at 400°C and 500°C yielded 40% and 13% conversion product, respectively, in a reaction time of 180 min. The results are summarized in Table 3; a graphical illustration is given in Figure 7.

Optimization of source of oxygen

The compatibility of the synthesized catalyst with different sources of oxygen such as dibenzoyl peroxide and hydrogen peroxide was tested. It was observed that there is a profound effect on the catalytic performance of the synthesized catalyst V_2O_5 (5%)-NiMnO calcined at 300°C when different sources of oxygen were employed. It was found that the catalyst displayed excellent performance with 100% conversion and >99% selectivity when molecular oxygen is used; while when dibenzoyl peroxide and hydrogen peroxide were used, the conversion product obtained was 17.75% and 5.31%,

Table 4 Effect of different sources of oxygen on the catalytic properties

Entry	Source	Conversion (%)
1	O_2	100
2	Dibenzoyl peroxide	17.75
3	Hydrogen peroxide	5.31

Reaction conditions: amount of catalyst 300 mg; reaction temperature 100°C; benzyl alcohol 2 mmol; toluene 10 mL; reaction time 2 h.

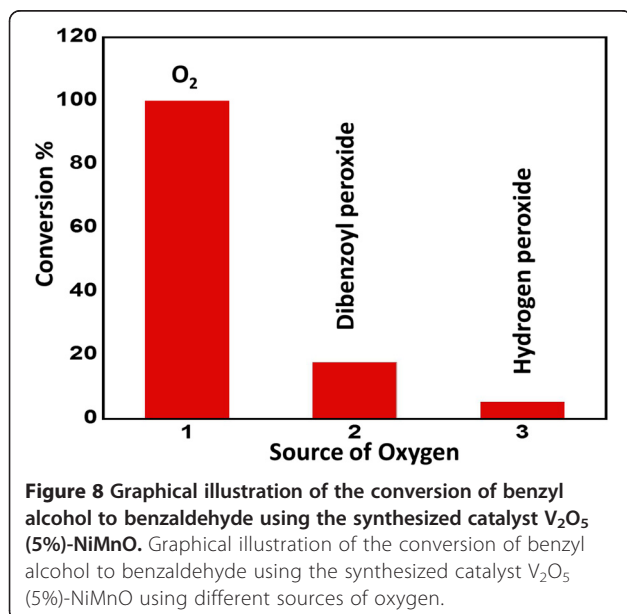


Table 5 Selective oxidation of benzyl alcohol and derivatives into corresponding aldehydes in the presence of O₂ as clean oxidant

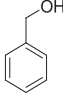
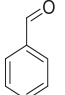
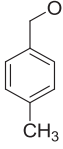
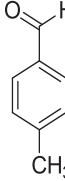
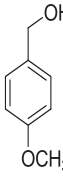
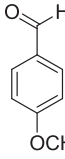
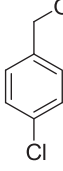
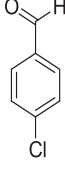
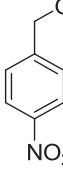
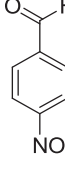
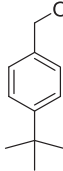
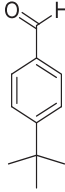
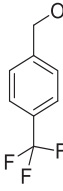
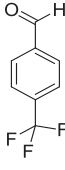
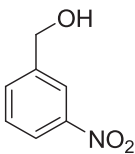
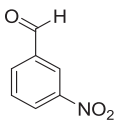
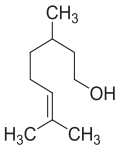
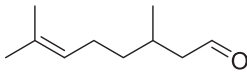
R. No.	Reactants	Products	Conversion (%)	Selectivity
1			100.00	>99
2			94.50	>99
3			89.36	>99
4			92.47	>99
5			100.00	>99
6			62.96	>99
7			59.32	>99

Table 5 Selective oxidation of benzyl alcohol and derivatives into corresponding aldehydes in the presence of O₂ as clean oxidant (Continued)

8			87.04	>99
9			4.07	>99

respectively. A graphical illustration is given in Figure 8. The results have been summarized in Table 4.

Catalytic performance on different substrates of benzyl alcohol

From the conversion of benzyl alcohol to benzaldehyde which was used as a model reaction, it was ascertained that the best catalytic activity was displayed by V₂O₅ (5%)-NiMnO, calcined at 300°C, which was established by spectral studies to contain a mixture of cubic hexanickel manganese(IV) oxide and orthorhombic dinickel dioxide hydroxide. It can be concluded that the catalyst with a large surface area and the presence of orthorhombic dinickel dioxide hydroxide on the surface of the catalyst plays a crucial role. It was confirmed that the surface area plays a crucial role in the catalytic performance as the catalysts calcined at other temperatures too and were found to possess cubic hexanickel manganese(IV) oxide and orthorhombic dinickel dioxide hydroxide, but it did come out as the best catalyst among the synthesized catalysts which could be due to the low surface area. It was also confirmed that the catalyst performs best in the presence of molecular oxygen as a source of oxygen. In order to determine the catalytic performance of V₂O₅ (5%)-NiMnO (300°C), the reaction was carried out under a similar set of conditions using a series of substituted benzyl alcohols, containing 4-CH₃, 4-OCH₃, 4-Cl, 4-NO₂, 4-C(CH₃)₃, 4-CF₃, and 3-NO₂ groups as different substrates, and their conversion to corresponding aldehydes was studied. It was found that the conversion product obtained was >60%, and selectivity displayed by the catalyst was >99%. It was observed that the catalyst selectively oxidizes aromatic alcohols, which was confirmed by the similar reaction carried out using citronellol as a substrate which yielded a conversion product of citronellal with 4%, unlike the results obtained from aromatic substrates. The results have been summarized in Table 5.

Conclusions

We have synthesized vanadia-supported nickel manganese mixed oxide catalyst using facile sol-gel chemistry. Nanovanadia-supported nickel manganese oxide shows high activity and stability for the oxidation of benzyl alcohol using molecular oxygen as a source of oxygen. A synergistic effect between optimum calcination temperatures and the chemical kinetics of the reaction was observed, and it was confirmed that calcination temperature plays an important role forming an active and durable catalyst. It can be believed that this catalyst can be further used for the evaluation of its oxidative property for the synthesis of other important aromatic and aliphatic aldehydes.

Competing interests

The authors declare that they have no competing interests.

Authors' contributions

SFA and MK2 designed the project and helped to draft the manuscript. SA and MK1 carried out the experimental part with synthesis and catalytic evaluation of the prepared material. NM, WT, and MNT carried out the characterization and interpretation of the results and also helped to draft the manuscript. AA and MRHS provided scientific guidance for successful completion of the project and also helped to draft the manuscript. All authors read and approved the final manuscript.

Acknowledgements

This project was supported by King Saud University, Deanship of Scientific Research, College of Science, Research Center.

Received: 14 December 2014 Accepted: 10 January 2015

Published online: 06 February 2015

References

- Nandi M, Mondal J, Sarkar K, Yamauchi Y, Bhaumik A. Highly ordered acid functionalized SBA-15: a novel organocatalyst for the preparation of xanthenes. *Chem Commun.* 2011;47:6677–9.
- Kuo I-J, Suzuki N, Yamauchi Y, Wu KC-W. Cellulose-to-HMF conversion using crystalline mesoporous titania and zirconia nanocatalysts in ionic liquid systems. *RSC Adv.* 2013;3:2028–34.
- Lee B-S, Huang L-C, Hong C-Y, Wang S-G, Hsu W-H, Yamauchi Y, et al. Synthesis of metal ion-histidine complex functionalized mesoporous silica

- nanocatalysts for enhanced light-free tooth bleaching. *Acta Biomater.* 2011;7(5):2276–84.
4. Oveis H, Rahighi S, Jiang X, Nemoto Y, Beitollahi A, Wakatsuki S, et al. Unusual antibacterial property of mesoporous titania films: drastic improvement by controlling surface area and crystallinity. *Chem Asian J.* 2010;5(9):1978–83.
 5. Carabineiro SAC, Bogdanchikova N, Pestryakov A, Tavares PB, Fernandes LSG, Figueiredo JL. Gold nanoparticles supported on magnesium oxide for CO oxidation. *Nanoscale Res Lett.* 2011;6(435):1–6.
 6. Sartipi S, Alberts M, Santos VP, Nasalevich M, Gascon J, Kapteijn F. Insights into the catalytic performance of mesoporous h-zsm-5-supported cobalt in Fischer–Tropsch synthesis. *Chem Cat Chem.* 2014;6(1):142–51.
 7. Lin J, Zhou Z, Li Z, Zhang C, Wang X, Wang K, et al. Biomimetic one-pot synthesis of gold nanoclusters/nanoparticles for targeted tumor cellular dual-modality imaging. *Nanoscale Res Lett.* 2013;8(170):1–7.
 8. Cao M, Wu D, Cao R. Recent advances in the stabilization of platinum electrocatalysts for fuel-cell reactions. *Chem Cat Chem.* 2014;6(1):26–45.
 9. Zaheer M, Hermannsdörfer J, Kretschmer WP, Motz G, Kempe R. Robust heterogeneous nickel catalysts with tailored porosity for the selective hydrogenolysis of aryl ethers. *Chem Cat Chem.* 2014;6(1):91–5.
 10. Gao B, Li Y, Shi N. Oxovanadium (IV) Schiff base complex immobilized on CPS microspheres as heterogeneous catalyst for aerobic selective oxidation of ethyl benzene to acetophenone. *React Funct Polym.* 2013;73(11):1573–9.
 11. Yang SC, Wang JQ. Catalytic oxidation of O-chlorotoluene to O-chlorobenzaldehyde by vanadium doped anatase mesoporous TiO₂. *Adv Mat Res.* 2013;781–784:182–5.
 12. Lee JK, Hong UG, Yoo Y, Cho YJ, Lee J, Chang H, et al. Oxidative dehydrogenation of n-butane over magnesium vanadate nano-catalysts supported on magnesia-zirconia: effect of vanadium content. *J Nanosci Nanotechnol.* 2013;13(12):8110–5.
 13. Hall N, Orio M, Jorge-Robin A, Gennaro B, Marchi-Delapierre C, Duboc C. Vanadium thiolate complexes for efficient and selective sulfoxidation catalysis: a mechanistic investigation. *Inorg Chem.* 2013;52(23):13424–31.
 14. Scholz J, Walter A, Ressler T. Influence of MgO-modified SBA-15 on the structure and catalytic activity of supported vanadium oxide catalysts. *J Catal.* 2014;309:105–14.
 15. Wang G, Lu X, Ling Y, Zhai T, Wang H, Tong Y, et al. LiCl/PVA gel electrolyte stabilizes vanadium oxide nanowire electrodes for pseudocapacitors. *ACS Nano.* 2012;6(11):10296–302.
 16. Tang Y, Rui X, Zhang Y, Lim TM, Dong Z, Hng HH, et al. Vanadium pentoxide cathode materials for high-performance lithium-ion batteries enabled by a hierarchical nanoflower structure *via* an electrochemical process. *J Mater Chem A.* 2013;1:82–8.
 17. Hoj M, Kessler T, Beato P, Jensen AD, Grunwaldt J-D. Structure, activity and kinetics of supported molybdenum oxide and mixed molybdenum–vanadium oxide catalysts prepared by flame spray pyrolysis for propane OHD. *Appl Catal A.* 2014;472:29–38.
 18. Raju G, Reddy BM, Park S-E. CO₂ promoted oxidative dehydrogenation of n-butane over VO_x/MO₂–ZrO₂ (M = Ce or Ti) catalysts. *J CO₂ Util.* 2014;5:41–6.
 19. Zhang H, Cao S, Zou Y, Wang Y-M, Zhou X, Shen Y, et al. Highly efficient V-Sb-O/SiO₂ catalyst with Sb atom-isolated VO_x species for oxidative dehydrogenation of propane to propene. *Catal Commun.* 2014;45:158–61.
 20. Verma A, Dwivedi R, Sharma P, Prasad R. Oxidative dehydrogenation of ethylbenzene to styrene over zirconium vanadate catalyst prepared by solution combustion method. *RSC Adv.* 2014;4:1799–807.
 21. Carrero CA, Keturakis CJ, Orrego A, Schomäcker R, Wachs IE. Anomalous reactivity of supported V₂O₅ nanoparticles for propane oxidative dehydrogenation: influence of the vanadium oxide precursor. *Dalton Trans.* 2013;42(35):12644–53.
 22. Ha NN, Huyen ND, Cam LM. Study on the role of SBA-15 in the oxidative dehydrogenation of n-butane over vanadia catalyst using density functional theory. *J Mol Model.* 2013;19(8):3233–43.
 23. Ballarini N, Battisti A, Cavani F, Cericola A, Lucarelli C, Racioppi S, et al. The oxygen-assisted transformation of propane to CO_x/H₂ through combined oxidation and WGS reactions catalyzed by vanadium oxide-based catalysts. *Catal Today.* 2006;116(3):313–23.
 24. Ballarini N, Battisti A, Cavani F, Cericola A, Cortelli C, Ferrari M, et al. The combination of propane partial oxidation and of WGS reaction in a single catalytic bed, and the self-adapting catalytic properties of vanadium oxide catalyst. *Appl Catal A.* 2006;307(1):148–55.
 25. Ksibi M, Elaloui E, Houas A, Moussa N. Diagnosis of deactivation sources for vanadium catalysts used in SO₂ oxidation reaction and optimization of vanadium extraction from deactivated catalysts. *Appl Surf Sci.* 2003;220(1–4):105–12.
 26. Danilevich EV, Popova GYA, Andrushkevich TV, Chesalov Yu A, Kaichev W, Saraev AA, et al. Preparation, active component and catalytic properties of supported vanadium catalysts in the reaction of formaldehyde oxidation to formic acid. *Stud Surf Sci Catal.* 2010;175:463–6.
 27. el Aakel L, Launay F, Atlamsani A, Brégeault JM. Efficient and selective catalytic oxidative cleavage of alpha-hydroxy ketones using vanadium-based HPA and dioxygen. *Chem Commun.* 2001;21:2218–9.
 28. Kirihara M. Aerobic oxidation of organic compounds catalyzed by vanadium compounds. *Coord Chem Rev.* 2011;255(19–20):2281–302.
 29. Čapek L, Adam J, Grygar T, Bulánek R, Vradman L, Košová-Kučerová G, et al. Oxidative dehydrogenation of ethane over vanadium supported on mesoporous materials of M41S family. *Appl Catal A.* 2008;342(1–2):99–106.
 30. Nouralishahi A, Khodadadi AA, Rashidi AM, Mortazavi Y. Vanadium oxide decorated carbon nanotubes as a promising support of Pt nanoparticles for methanol electro-oxidation reaction. *J Colloid Interface Sci.* 2013;393:291–9.
 31. Gawande MB, Pandey RK, Jayaram RV. Role of mixed metal oxides in catalysis science-versatile applications in organic synthesis. *Catal Sci Technol.* 2012;2:1113–25.
 32. Wan Y, Zhao W, Tang Y, Li L, Wang H, Cui Y, et al. Ni-Mn bi-metal oxide catalysts for the low temperature SCR removal of NO with NH₃. *Appl Catal B.* 2014;148–149:114–22.
 33. Huang L, Zhang F, Chen R, Hsu AT. Manganese-promoted nickel/alumina catalysts for hydrogen production via auto-thermal reforming of ethanol. *Int J Hydrogen energy.* 2012;37(21):15908–13.
 34. Koike M, Ishikawa C, Li D, Wang L, Nakagawa Y, Tomishige K. Catalytic performance of manganese-promoted nickel catalysts for the steam reforming of tar from biomass pyrolysis to synthesis gas. *Fuel.* 2013;103:122–9.
 35. Zhang Y, Qin Z, Wang G, Zhu H, Dong M, Li S, et al. Catalytic performance of MnOx–NiO composite oxide in lean methane combustion at low temperature. *Appl Catal B.* 2013;129:172–81.
 36. El-Refaei SM, Saleh MM, Awad MI. Enhanced glucose electrooxidation at a binary catalyst of manganese and nickel oxides modified glassy carbon electrode. *J Power Sources.* 2013;223:125–8.
 37. Adil SF, Assal ME, Khan M, Al-Warthan A, Siddiqui MRH. Nano silver-doped manganese oxide as catalyst for oxidation of benzyl alcohol and its derivatives: synthesis, characterisation, thermal study and evaluation of catalytic properties. *Oxid Commun.* 2013;36(3):778–91.
 38. Siddiqui MRH, Warad I, Adil SF, Mahfouz RM, Al-Arifi A. Nano-gold supported nickel manganese oxide: synthesis, characterisation and evaluation as oxidation catalyst. *Oxid Commun.* 2012;35(2):476–81.
 39. Silversmit G, Depla D, Poelman H, Marin GB, Gryse RD. Determination of the V2p XPS binding energies for different vanadium oxidation states (V⁵⁺ to V⁰⁺). *J Electron Spectrosc.* 2004;135(2–3):167–75.
 40. Biesinger MC, Payne BP, Grosvenor AP, Lau LWM, Gerson AR, Smart RSC. Resolving surface chemical states in XPS analysis of first row transition metals, oxides and hydroxides: Cr, Mn, Fe, Co and Ni *Appl Surf Sci.* 2011;257(7):2717–30.
 41. Biesinger MC, Payne BP, Lau LWM, Gerson A, Smart RSC. X-ray photoelectron spectroscopic chemical state quantification of mixed nickel metal, oxide and hydroxide systems. *Surf Interface Anal.* 2009;41(4):324–32.
 42. Al-Fatesh ASA, Fakeeha AH. Effects of calcination and activation temperature on dry reforming catalysts. *J Saudi Chem Soc.* 2012;16(1):55–61.

Submit your manuscript to a SpringerOpen® journal and benefit from:

- Convenient online submission
- Rigorous peer review
- Immediate publication on acceptance
- Open access: articles freely available online
- High visibility within the field
- Retaining the copyright to your article

Submit your next manuscript at ► springeropen.com